

Optical Measurements

Paper 15

***TREATMENT OF L2F MEASUREMENT
VOLUME DISTORTIONS CREATED BY
CURVED WINDOWS***

X. Ottavy, I. Trebinjac, A. Vouillarmet

*Laboratoire de Mécanique des Fluides et d'Acoustique
Ecole Centrale de Lyon
F-69131 Ecully cedex*

Treatment of L2F Measurement Volume Distortions created by Curved Windows

X. OTTAVY, I. TREBINJAC and A. VOUILLARMET

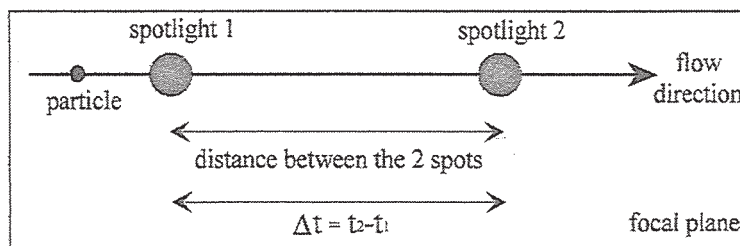
*Laboratoire de Mécanique des Fluides et d'Acoustique
UMR CNRS 5509 / ECL / UCB Lyon 1
Ecole Centrale de Lyon - BP 163 - 69131 Ecully cedex - France*

Introduction

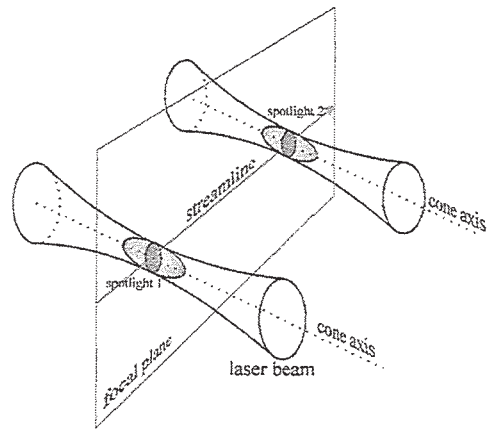
The state of art transonic compressor evolves into low aspect ratios, and highly loaded configurations where complex phenomena dominate the flow field. Therefore, there is a great interest in acquiring detailed 3D measurements. Laser « two focus » (L2F) anemometry answers this need, all the more it excels in areas of high spatial selectivity that enables measurements near surfaces. Optical access to the inter-blade flow field is typically provided by thick, flat glass windows. This results in a mismatch between the window surface and the true shroud contour. In order to maintain the proper impeller tip clearance, curved windows can be used. But the curvatures lead to optical distortions of the laser beams passing through the windows. Judging from the works of M. D. Hathaway and P. Wernet [1,2], in case of laser Doppler anemometry, the distortions do not prevent acquiring data but lead to an increase of uncertainty in the measurement. In case of L2F anemometry, the distortion hinders the creation of acceptable foci. A study of these distortions is presented hereafter, and an optical assembly to restore acceptable foci is proposed.

Principle of the L2F-2D laser anemometry

The principle of the L2F-2D laser anemometry consists in measuring the time of flight of small particles (mixed in the flow) when they cover a distance fixed by two spotlights. A particle passing through both spotlights produces two successive pulses of scattered light. The measurement of the elapsed time between the pulses yields the particle velocity value.



Each spotlight is created by a focused laser light beam using a lens. The volume of each focus is assimilated with an ellipsoid whose characteristic sizes are small compared with the gap between the two foci. So, to have a good accuracy and a high light concentration, a minimum size of the focus volume has to be preserved.



Optical distortions of the laser beam passing through windows

Let's take the reference case where the light beam doesn't pass through any glass window and then let us assume each focus is a geometric point F that is the top of the incident light cone where the frontal lens of the optical system is its base.

The three figures (1,2,3) show the light surfaces (S_1 , S_2) included in the light cone which are perpendicular to the (x,y) plane. The point I is the intersection between the window surface and the axis of the cone light $[FI]$.

First, let's look at the case represented in figure 1. When the laser cone passes through a plane window which thickness is e_1 , the focused spot F remains very similar to a geometric point. This consideration is true when the top light cone angle is small (for example around 5°).

Let us now replace the plane window by an equal thickness curved glass that is shaped on a r_1 radius cylinder whose axis is parallel to the (o,z) direction, as shown in figure 2. Two concentrated light zones $[F_1F'_1]$ and $[F_2F'_2]$ appear. The light surfaces (S_1 , S_2) focus on $[F_2F'_2]$ where F is the mid-point. Because of the window curvature, the angle between the cone axis and these surfaces is greater than in the case of the flat glass. Thus, the light surfaces do not intersect one another at their foci, like in the case of a plane window, but intersect at $[F_1F'_1]$. If one now looks at the light surfaces perpendicular to the (o,z) direction, they focus on $[F_1F'_1]$ and intersect one another at $[F_2F'_2]$. Consequently, $[F_1F'_1]$ and $[F_2F'_2]$ are two focus zones which diverge when r_1 decreases and the thickness e_1 increases. Typically for $r_1=250$ mm, $e_1=2.8$ mm and an 80 mm immersion (FI distance), the gap between these two zones is around 0.5 mm. That highlights the uncertainty problems caused by the defocusing of the probe volume.

As shown in figure 3, to prevent this measurement volume distortion, we are inserting a second window between the curved laser window and the frontal lens to create in the (x,y) plane the same distortions as in the (x,z) plane. The second window is a e_2 thick curved glass shaped on a r_2 radius cylinder whose axis is parallel to the (o,y) direction. The radius r_2 and the thickness e_2 being chosen, the distance between the two windows is adjusted in order to bring the two focus zones nearer

together. Thus, the distortions created by the curvature in the (x,y) plane and the distortions created by the curvature in the (x,z) plane counterbalance each other. There is an optimal adjustment that leads to a focus which is comparable to a point F_3 . Typically for the previous configuration, if $r_1=250$ mm, $e_1=2.8$ mm, $r_2=250$ mm and $e_2=2.1$ mm, the calculation predicts an optimal distance between the two windows equal to 39 mm.

When acquiring some data in a compressor, the laser beam is often not perpendicular to the shroud glass window. Because of the geometry of the meridional section, we define an angle, called Φ_1 , between the laser cone axis and the perpendicular vector of the window surface. Due to the blade geometry (problems of shadow regions due to blade twist) we define the η_1 angle in the azimuthal plane.

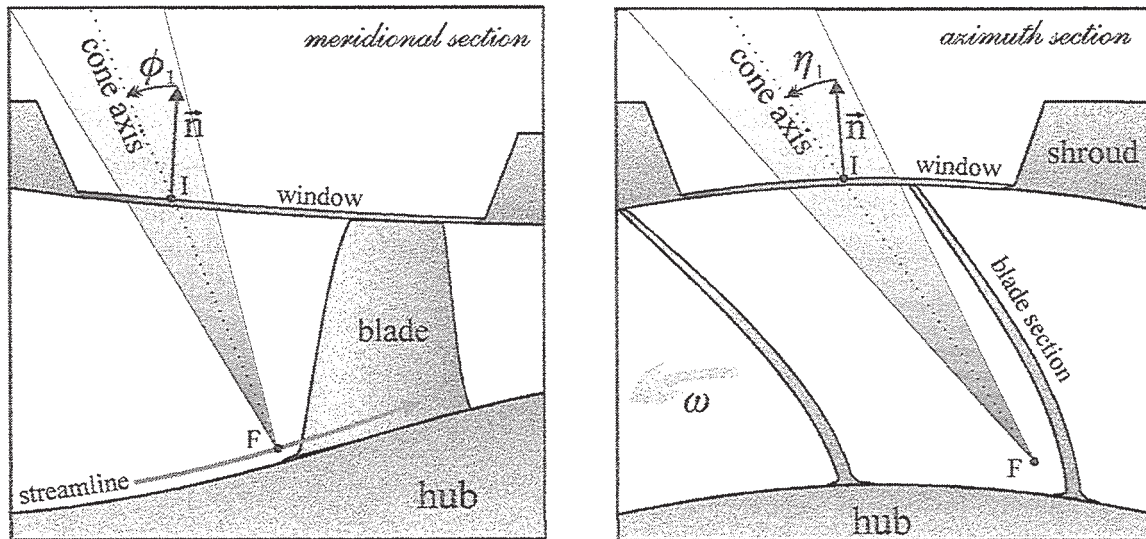


Figure 4

Even if the laser beam axis is not perpendicular to the shroud window, the same methodology is applied, but the orientation of the second curved window has to be adapted.

There are five parameters which characterize the inserted window :

- r_2 : the radius of the inserted window.
- e_2 : the thickness of the inserted window.
- d : the distance between the two windows.
- η_2, Φ_2 : the orientation angles of the inserted window (equal 0,0 if the η_1, Φ_1 values equal 0,0).

Thus, we have developed a numerical simulation to predict the different parameter values which will optimize the optical configuration.

Numerical simulation

Discretization of the light cone

Figure 5 represents a section of the light beam cone whose top angle equals 5° . Circles, characterized by a I center and a r_i radius, which are the trace of n smaller cones included in the laser light cone are observed. The different values of the r_i radii lead to the determination of the θ_i top angle of these cones (figure 6). Each radius is fixed in order to equalize all the cell surface areas (ds_i). Then, the light power per cell is set to the light intensity of this cell. Due to the Gaussian distribution of the light intensity on the cone base, the Pow_i light power for a cell is calculated :

$$Pow_i = \frac{I_{max} \cdot \Pi \cdot r_0^2}{2 \cdot m} \cdot \left(e^{-2 \cdot \frac{r_{i+1}^2}{r_0^2}} - e^{-2 \cdot \frac{r_i^2}{r_0^2}} \right)$$

$$\text{with } \begin{cases} I(\theta = 0^\circ) = I(r = 0) = I_{max} \\ I(\theta = 5^\circ) = I(r = r_0) = I_{max} / e^2 \end{cases}$$

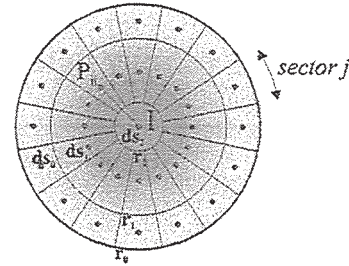
m : number of angular sectors.

Each cell is represented by a P_{ij} point whose polar coordinates are $r_{P_{ij}} = (r_{i+1} + r_i)/2$ and $\alpha_j = j \cdot 2 \cdot \pi / m$. The volume of the laser cone is then discretized by a set of straight lines connecting F to P_{ij} points. Each straight line defines a light beam which has a prescribed light power (calculated above) and a prescribed thickness (which has been kept constant at $8 \mu\text{m}$, because it is the approximate value of one spot diameter of the probe volume).

In our calculation, the number of P_{ij} points equals 49 ($= n \times m + 1 = 3 \times 16 + 1$).

Calculation of the optical pass and of focusing

To start the calculation the reference case (without any window) is used to discretize the laser cone. Then the different glass windows are inserted and the calculation of the optical pass of each light beam passing through the windows is done, based on Descartes's law. Knowing the spatial orientation of each straight line after they passed through the windows, the intersections between one beam and all the others (and this for each beam) are calculated. One intersection point position is, in fact, defined as the mid-point of the smallest distance between two straight lines.



$$ds_0 = ds_1 = ds_2 = ds_i$$

Figure 5

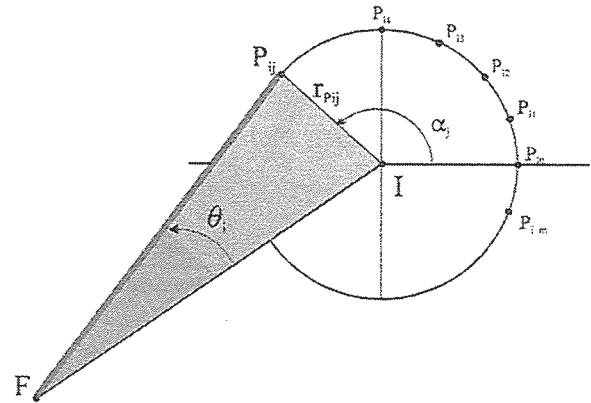


Figure 6

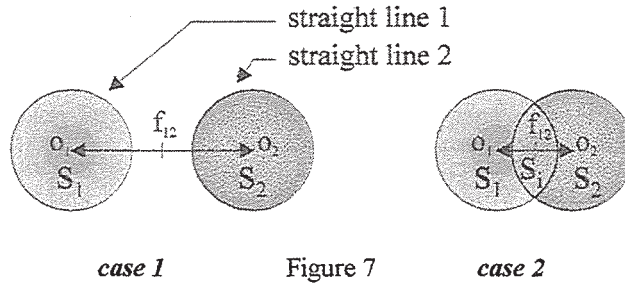


Figure 7
 (o_1o_2) = smallest distance between two straight lines (1 and 2).
 f_{12} = intersection point.

In figure 7, two cases are drawn in a plane perpendicular to the cone axis. The case 1 represents two cylindrical light beams which never intersect one another. The P_f light power of the intersection point is then set to zero. In the case 2, there is an intersection surface (S_i) between the two cylindrical light beams. The light power of the intersection point is calculated by :

$$P_f = \frac{S_i}{S_1} \cdot Pow_1 + \frac{S_i}{S_2} \cdot Pow_2$$

Then, the barycentre of this set of points shaping the focus spotlight is calculated, weighted by the light power of each point. This enables to get the axial and transversal standard deviations which lead to the characteristic sizes of the focus volume.

$$\sigma_x = \sqrt{\frac{\sum_1^{Nbpoint} P_{fi} \cdot (\bar{X} - X_i)^2}{\sum_1^{Nbpoint} P_{fi}}} \quad \sigma_t = \sqrt{\sigma_y^2 + \sigma_z^2} = \sqrt{\frac{\sum_1^{Nbpoint} P_{fi} \cdot (\bar{Y} - Y_i)^2}{\sum_1^{Nbpoint} P_{fi}} + \frac{\sum_1^{Nbpoint} P_{fi} \cdot (\bar{Z} - Z_i)^2}{\sum_1^{Nbpoint} P_{fi}}}$$

with Nbpoint = number of intersection points.

Optimisation

For a given optical configuration, the calculation predicts the characteristic sizes of the focus volume. Then, it optimizes the different parameter values of the inserted window, in minimizing the axial characteristic size of the focus volume.

Results and application

The transonic compressor ECL4

All this study have been applied in the case of the axial transonic compressor ECL4 designed and built by SNECMA, in order to acquire detailed data of the flow field, using a L2F-2D laser anemometer. The feature of the shroud glass window is defined by the characteristics of the compressor, i.e. its radius is fixed by the geometry of the shroud contour and its thickness by the pressure of the flow field (this thickness has to be minimized in order to minimize the optical

distortions). Due to the geometric and pressure characteristics of the ECL4 compressor, a curved shroud glass window with a 253 mm radius and a 2.9 mm thickness is used.

Choice of the inserted window parameters

How to choose the inserted window e_2 thickness and r_2 radius, and the d distance between the two glasses ? Let's take the configuration where the laser beam is perpendicular to the shroud window surface.

In figure 8, the σ_x distribution is represented as a function of the r_2 inserted window radius, for a e_2 fixed thickness and a $[FI]$ given immersion (distance between the probe volume and the shroud surface). The curves are plotted for several d values (distances between the two glass windows). For any d distance, it always exists a r_2 value for which σ_x reaches a minimum value and on the other way around. Moreover, for all the curves, the minimum values of σ_x are equal.

In figure 9, the σ_x distribution is plotted versus the e_2 inserted window thickness, for various $[FI]$ immersions of the probe volume, at a prescribed r_2 value. As seen before, at any r_2 values corresponds an optimization of the d value leading to a minimum σ_x . Each point of these curves results from this optimization of the d value. For any other prescribed r_2 value, the curves will be similar, because all σ_x minima are the same (c.f. figure 8). For a fixed immersion of the probe volume, there is a value of the thickness leading to an optimal value of σ_x . If data have to be acquired for several immersions, the e_2 thickness is fixed by the deepest immersion. In our configuration, where immersion ranges from 80 to 20 mm, these curves lead to a choice of **$e_2=1.8$ mm**.

Using that e_2 thickness value, the curves in figure 8 have to be replotted, in order to have the relation $r_2=f(d)$ for a given immersion. The d distance must not exceed a maximal value equal to the focus distance of the lens minus the immersion of the probe volume. However, for given r_2 and e_2 , the d distance is an increasing function of the immersion. Thus, the focus distance of the lens (270 mm) and the maximum immersion (80 mm) lead to a maximal distance : $d_{max}=190$ mm. The radius of the inserted window is thus determined, using the replotted figure 8 ; it leads to **$r_2=470$ mm**.

At last, the d distance between the two glass windows is optimized for each immersion (figure 10).

Moreover, in the case of a non zero incident angle, the calculation predicts optimal angles for the orientation of the inserted window (η_2, Φ_2).

Shape of the focus volume

The predicted shape of the focus volume is represented (figure 11) for an example where the laser beam has an Φ_1 incident angle which equals 10° ($\eta_1=0^\circ$). The geometric point is shown in the

reference case. The focus shape looks to be better in the case of the 2 curved windows than in the case of one plane window. The case with only one curved window is not represented here because its focus volume is much larger ($\sigma_x=250 \mu\text{m}$) than the focus volume obtained with two curved glasses. We observed the focus spots visible under the microscope and noted that their shape was the predicted one.

Conclusion

The inserted window provides good results. To restore acceptable foci, it is a simple and an economical solution which, most of the time and particularly in the complex cases, leads to better results than using only one plane window.

The numerical simulation has been developed using the Windows environment which enables the dialogue between other programs like this of the calculation of the shadow regions or the acquiring program. Thus, it results in an improvement of the acquired conditions (investigated zones, acquired time, user-friendliness, ...).

Moreover, this optical assembly would be interesting in the case of L2F-3D where each laser beam axis has a non-zero incident angle. The optimization of the measurement volume will result from a compromise between individual optimal solutions obtained for each incident laser cone.

References

- [1] M. D. Hathaway, R. M. Chriss, J. R. Wood, A. J. Strazisar, « Experimental and Computational Investigation of the NASA Low Speed Centrifugal Compressor Flow Field », in *Journal of Turbomachinery*, July 1993, Vol. 115/527.
- [2] P. Wernet & J. Skoch, « A 4-Spot Time-of-Flight Anemometer for Small Centrifugal Compressor Velocity Measurements », in *Proceedings on the Sixth International Symposium on the Application of Laser Techniques to Fluid Mechanics*, Lisbon, July 20-23, 1992.

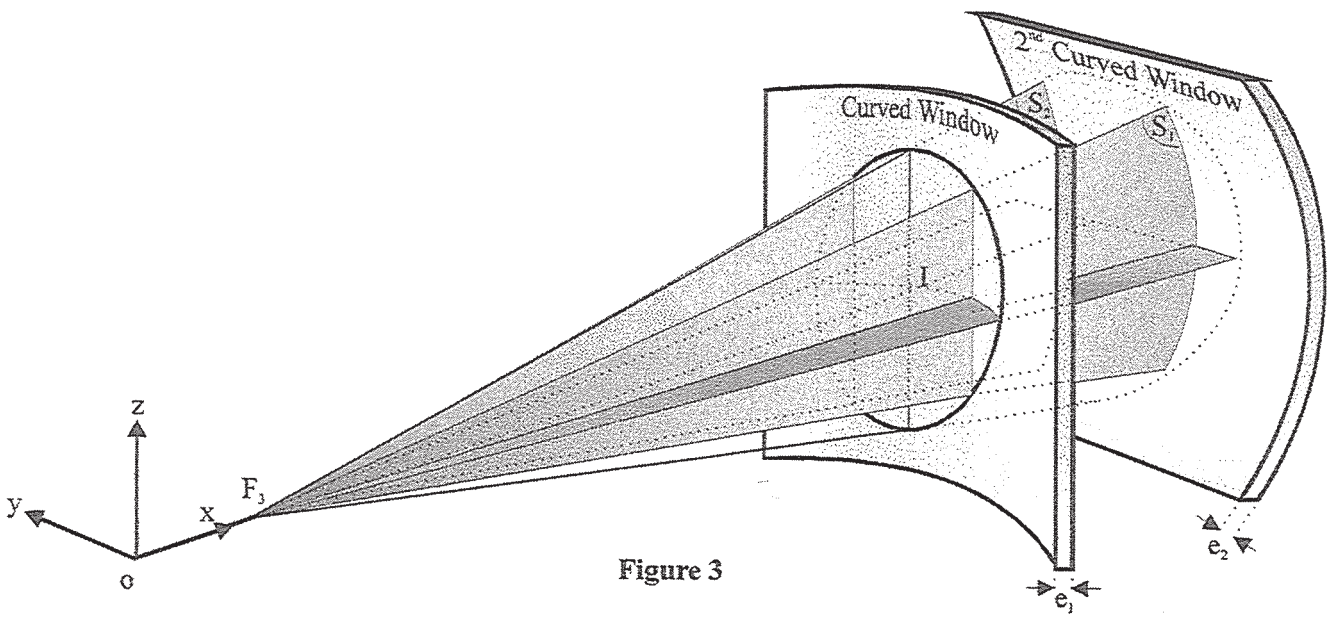
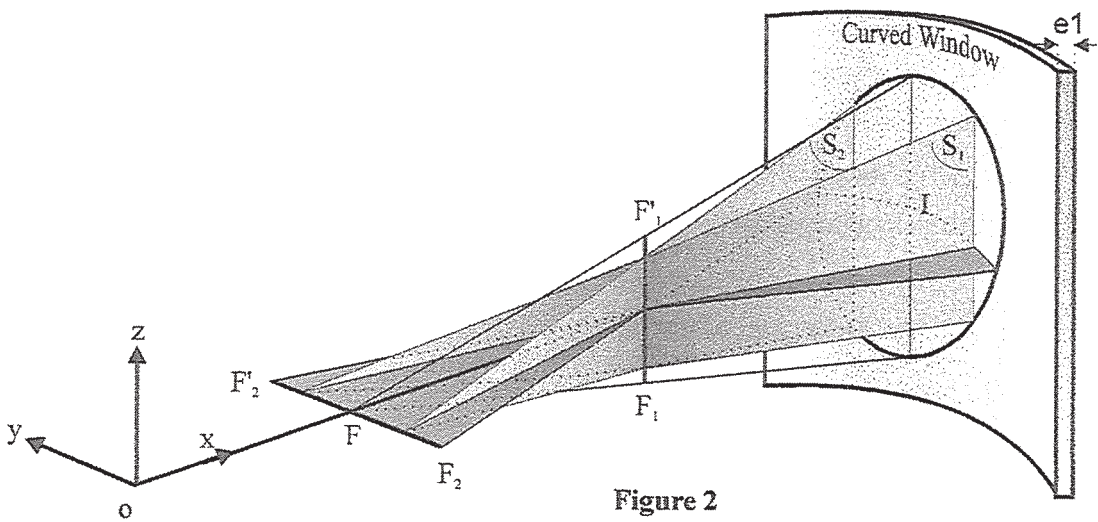
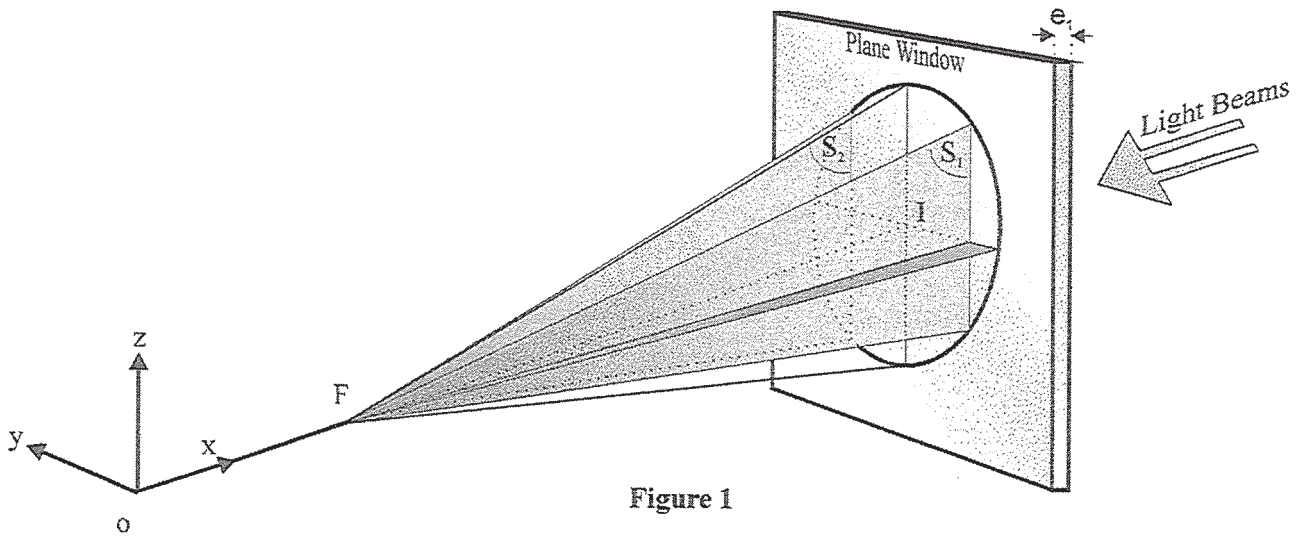


Figure 8 : sigma distribution as a function of the inserted window radius, for several distances between the two windows ($r_1=253$, $e_1=2.9$, e_2 value and FI immersion fixed).

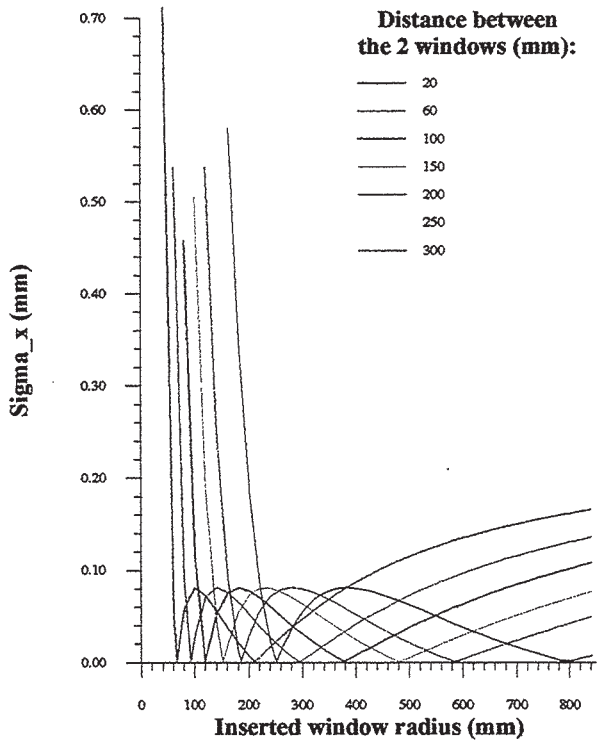


Figure 9 : sigma distribution as a function of the inserted window thickness, for several immersions of the probe volume ($r_1=253$, $e_1=2.9$, whatever the r_2 value is, the distance between the two windows being optimized for each point).

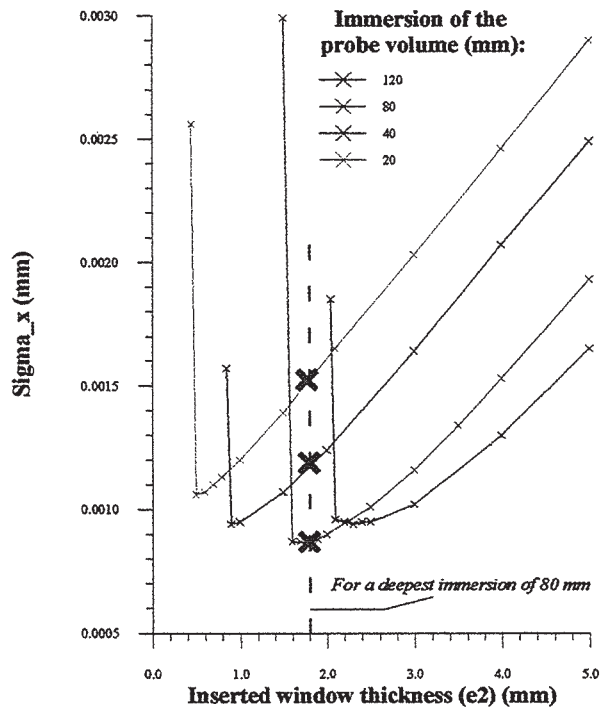


Figure 10: distance between the two windows distribution as a function of the immersion ($r_1=253$, $e_1=2.9$, $r_2=470$, $e_2=1.8$).

